CORPUS PUBLISHERS

Current Trends in Engineering Science (CTES)

ISSN: 2833-356X

Volume 5 Issue 1, 2025

Article Information

Received date : June 02, 2025

Published date: June 19, 2025

*Corresponding author

Maria Adrina Paixão de Souza da Silva, Institute of Technology, Federal University of Pará, Brazil

DOI: 10.54026/CTES/1075

Keywords

Aluminum alloys; Cutting temperature; Machinability; Thermal analysis

Research Article

Non-Linear Thermal Response in Necking Tests of an Al-Si Alloy: A Combined Geometric and Statistical Approach

Rafael de Araújo Ribeiro[1], Emerson Rodrigues Prazeres[2], Nádia Silva Cosmo[2], Leonardo Carvalho de Oliveira[2], Amanda Lucena de Medeiros[2], Thiago Antônio Paixão de Sousa Costa[3] and Maria Adrina Paixão de Souza da Silva[2*]

[1]*University of Waterloo, U. WATERLOO, Canadá*

[2]*Institute of Technology, Federal University of Pará, Brazil*

[3]*Federal Institute of Pará, Marco, Brazil*

Abstract

Light metals and their alloys, especially aluminum alloys because of their good strength/weight ratio, have been used in the automotive and aerospace industries to reduce the amount of fuel required and consequently the amount of energy, in a worldwide effort to save energy resources. As mentioned above, among the alloys, the aluminum-silicon binary (Al-Si) stands out, as it is used in the construction of mechanical parts of automobiles and the aeronautical industry in the structure of airplane wings. In the automotive industry, components made from the Al-Si alloy need to be machined for their final application and, therefore, this implies in-depth knowledge of the machinability of such alloys, to estimate the machining parameters that require less energy expenditure and provide better surface finish of the part with less tool wear. The present study determined the dependence of the solidification parameters and alloy composition on the machinability of the material, as well as specified parameters for measuring the machining temperature during necking tests.

Introduction

Al-Si alloys are widely used in the automotive and aerospace industries due to their low density, good castability, corrosion resistance, and satisfactory mechanical properties. The combination of aluminum and silicon results in complex microstructures composed of both eutectic and primary phases, which significantly influence machinability, wear resistance, and the thermal response of the material during cutting. In particular, the silicon content plays a decisive role: while hypoeutectic alloys favor improved machinability, hypereutectic alloys generally exhibit higher hardness and increased tool wear [1].

An increase in silicon content - from 6% up to 18% by weight- affects particle morphology and drastically alters the material's behavior during machining, influencing parameters such as thrust force, surface roughness, and burr formation [1]. Therefore, investigating cutting temperature as an indicator of thermal regime is essential, as temperature fluctuations affect not only tool integrity but also surface quality and process stability.

The study of temperature in machining processes has long been acknowledged as a key factor in tool wear, surface integrity, and process optimization. It is well established that over 90% of the mechanical energy in machining is converted into heat, most of which concentrates near the cutting edge, leading to rapid tool degradation under unfavorable conditions [2-6]. Since the early experiments of Count Rumford in the 18th century and the pioneering studies by Taylor, Shore, and Herbert in the early 20th century, a variety of analytical and experimental methods have been proposed to measure and model temperature in cutting operations [2,3].

Cutting temperature is primarily influenced by cutting speed, feed rate, depth of cutting, and material properties. As cutting speed increases, heat generation intensifies, often resulting in plastic softening, reduced tool life, and dimensional inaccuracies due to thermal expansion. Models by Trigger & Chao and Loewen & Shaw have quantified how energy generated from plastic deformation and friction is partitioned between the chip, the tool, and the workpiece, enabling better prediction of thermal fields in the cutting zone [2-6].

Experimental techniques such as tool-work thermocouples, embedded thermocouples, infrared sensors, and thermal paints have been applied to determine cutting temperatures with varying degrees of precision and intrusiveness. It is also noted that the highest temperatures often occur in the secondary shear zone -at the chip-tool interface - where heat is generated primarily by sliding friction [2-3,6]. These thermal conditions directly influence tool wear mechanisms and define the limits of feasible cutting parameters.

In this context, analyzing thermal conditions during a necking test of Al-Si alloys represents a promising approach to understanding operating regimes under variable geometry and rotation. Similar studies performed on A390 alloys using minimum quantity lubrication (MQL) with nanofluids demonstrated that cutting speed and feed rate are critical factors in surface roughness and directly impact interface heating [6].

Additionally, recent studies on A356 alloys highlight that microstructural refinement—driven by solidification velocity - directly affects mechanical properties, particularly in alloys cast under low pressure and subjected to T6 heat treatment. The secondary dendrite arm spacing (λ_2) is strongly correlated with mechanical strength, as demonstrated in simulations and tensile tests conducted on automotive wheels [7]. Predictive modeling using Hall-Petch and Ludvig equations has proven effective in estimating mechanical performance based on λ_2 [7].

Moreover, investigations into silicon morphology in alloys such as B319 have shown that electrical conductivity and mechanical resistance are influenced by distinct microstructural mechanisms. The modification of eutectic silicon - through strontium additions and solidification rate adjustments—has proven effective in enhancing conductivity without compromising strength [8]. These findings reinforce the importance of analyses that integrate thermal, structural, and machining properties in Al-Si alloys, especially under non-conventional geometries like the one investigated in this study.

This work investigates the thermal behavior during a necking test in a variable-geometry Al-8%Si alloy sample cast in a metal mold. The approach includes modeling the diameter as a function of time, calculating the corresponding cutting speed, and conducting statistical and graphical analyses of temperature evolution, including 3D visualizations and correlations with geometric and temporal parameters. The findings aim to support machining parameter optimization and deepen the understanding of thermal mechanisms in dimensionally dynamic cutting operations.

Materials and Methods

Preparation of the metallic alloy

Initially, aluminum ingots were sectioned into small segments to facilitate melting. These segments were melted in a BRASIMET muffle furnace, enabling the extraction of small samples for chemical analysis via the first casting. After this initial melting, the chemical composition of the base material was determined. From these results, the required mass percentage of alloying elements was calculated to achieve the target composition. For precise weighing, an OHAUS Adventurer analytical balance was used, offering a resolution of 0.01 g.

Permanent mold (coquille)

The alloy casting was performed using a metallic permanent mold (Figure 1a), composed of two steel halves aligned and bolted to form a cylindrical cavity with a diameter of 22 mm. Prior to casting, the mold was ground (Figure 1b) and coated with a kaolin-based slurry (Figure 1c). The use of U-shaped molds plays a crucial role in controlling the microstructure and mechanical properties of cast metal alloys. This geometry promotes uniform heat extraction, enabling more controlled and directional solidification, which helps reduce internal defects such as porosity, shrinkage cracks, and segregation. The U-shape also facilitates unidirectional solidification, allowing liquid metal to feed the advancing solidification front and minimizing structural flaws. An optimized cooling rate in the U-mold leads to the formation of finer and more homogeneous grains, enhancing the mechanical strength and integrity of the part. Consequently, this mold design enables the production of components with improved structural performance, a more uniform microstructure, and fewer casting defects [9,10].

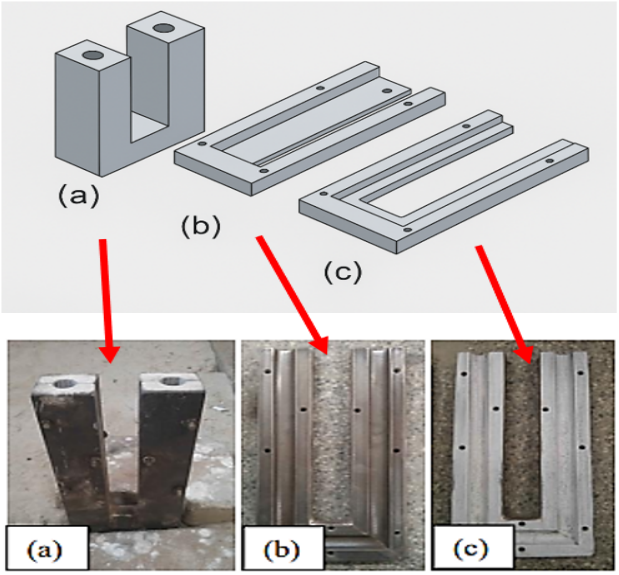

Figure 1: Metallic mold used for alloy production: (a) assembled mold, (b) sanded surface, and (c) mold coated with kaolin.

Immediately before casting, the mold was preheated to 250°C to remove internal moisture and ensure complete mold filling by the molten metal. The molten metal was poured into the mold by gravity. Once solidification was complete, the mold was disassembled, and the solidified part was removed.

Melting and solidification

After the raw materials were prepared, the crucible used for melting was preheated to 200°C in the furnace. It was then removed and coated internally with kaolin to reduce metal adhesion. The weighed aluminum and silicon were placed into the crucible, which was then returned to the furnace set to 1000°C to melt the contents. This temperature was maintained for 1 hour and 30 minutes. Upon confirming complete melting, the crucible was withdrawn and placed on a refractory base.

The molten alloy was then manually stirred using a steel spatula to ensure homogenization. Subsequently, an inert argon gas flow (0.2 L/s) was introduced for approximately 1 minute through a stainless-steel tube connected to a $10m^3$ cylinder. This degassing step aimed to remove low-density inclusions and dissolved gases, resulting in slag formation on the bath surface, which was manually removed.

A sample for chemical analysis (witness sample) was immediately cast in a preconditioned steel mold (sanded, preheated, and coated with kaolin solution). A thermocouple was then inserted into the crucible to monitor the temperature until it reached approximately 730°C, the targeted pouring temperature. At this point, the alloy was poured into the prepared permanent molds. After solidification, two types of samples were obtained: the U-shaped test piece (Figure 2a) and the chemical analysis sample (Figure 2b).

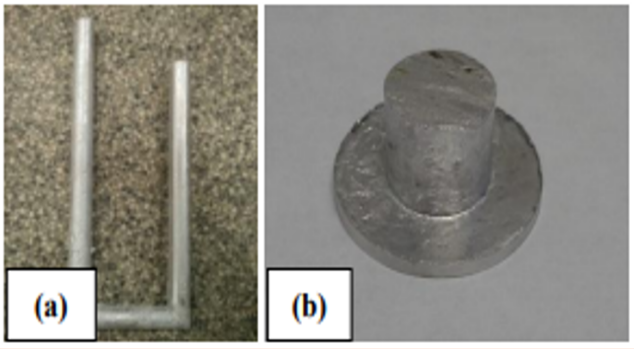

Figure 2: (a) Cast U-shaped ingot and (b) sample for chemical analysis.

Chemical analysis

The chemical composition of the alloy was determined using a Bruker Q4 TASMAN Optical Emission Spectrometer. Three burns were conducted on the witness sample to ensure repeatability and reliability of results. The data obtained are presented in Table 1.

Table 1: Chemical composition of the studied alloy.

Analysis No.	Al wt%	Si wt%
1	91,53	8,222
2	91,61	8,146
3	91,56	8,163
Average	91,58	8,177

Machining test (necking)

The machinability of the alloy was evaluated using a necking test, in which the specimen was subjected to a single-pass longitudinal cut performed on a conventional NARDINI lathe. The choice of the necking method is based on its relevance to industrial applications and its ability to simulate machining conditions where the entire cross-section is progressively removed. This approach enables the evaluation of the influence of geometry and material behavior on thermal response during cutting.

As a cutting tool, a ROCAST HSS 12 chisel was used, with dimensions ¾" × ⅛" × 6" (Figure 3), mounted on a PB-852 STD ¾" straight tool holder. The tool was used in its original condition - unsharpened and unpolished. During the necking process, the cutting temperature was measured every second using a FLIR E40 infrared thermometer (Figure 3), connected to a notebook for real-time data acquisition. The recorded temperature data were later processed to eliminate possible noise due to distance variation or vibrations affecting the sensor, yielding smooth cutting temperature profile over time.

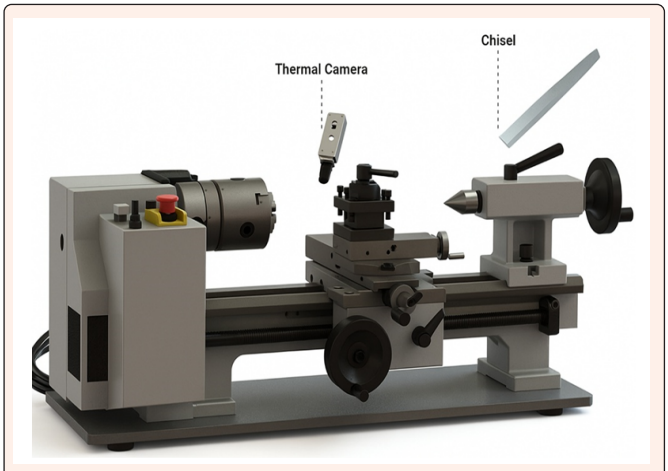

Figure 3: Thermal data acquisition system using infrared thermometer. Adapted from [11].

The machining parameters adopted included a feed rate of 0.094 mm/rev and a variable cutting depth determined by the cross-sectional geometry of the specimen. Based on standard values for aluminum alloys machined with high-speed steel tools, the spindle rotation was set to 630 rpm, yielding an average cutting speed in the range typical for roughing operations.

This experimental configuration aligns with previous studies in which dry necking operations were used to assess the machinability of directionally solidified metallic alloys. The necking method enables the observation of heating phenomena throughout the cut, reflecting the effects of macrostructural and microstructural features on the tool-workpiece thermal interaction. The temperature evolution thus serves as a proxy for evaluating machinability under transient conditions imposed by variable geometry, as also reported by [4] and [11].

Modeling and statistical analysis

Modeling of geometry and process variables

The specimen's geometry resulted in a continuous variation of diameter (D), in millimeters (mm), throughout the necking test. This variation was modeled using the Equation 1:

$$D(t) = 19.3 - 0.07924 \times t \qquad (Eq.1)$$

Based on this, the theoretical cutting speed (VC), in m/min, was calculated according Equation 2:

$$V_c(t) = \frac{(n\pi D(t))}{1000} \qquad (Eq.2)$$

Considering n = 630 rpm, the cutting speed was also converted to mm/s to facilitate statistical analysis.

Descriptive statistical analysis

Measures of central tendency (mean) and dispersion (variance and standard deviation) were applied to the main variables of interest: cutting temperature, diameter, and cutting speed. These statistics allowed for the evaluation of data consistency and the identification of the process's thermal behavior and stability.

Correlation between variables

Pearson correlation coefficients were calculated between the following combinations:
- Temperature (T) × Cutting speed (VC) × Diameter (D)
- Temperature (T) × Cutting speed (VC) × Time (t)

The results were used to compare the physical influence (geometry and speed) against the temporal evolution of the process.

Results and Discussion

The analysis of cutting temperature revealed non-linear behavior throughout the necking test. A peak temperature of approximately 46°C was observed, followed by a gradual decline. A linear correlation between temperature and time yielded a coefficient of determination (R^2) of 0.38, indicating a weak linear relationship. However, when a second-degree polynomial model was applied, the fit improved significantly, resulting in $R^2 > 0.93$. This reflects the non-linear thermal response as the material volume being cut and the contact conditions evolve during the process.

Data obtained from supplementary tests at different spindle speeds confirmed this trend: higher spindle speeds generated more pronounced temperature peaks, while intermediate speeds tended to yield greater thermal stability [12].

A histogram of the recorded temperatures indicated a predominant thermal regime between 43°C and 46°C (Figure 4). Notably, the standard deviation of the temperatures decreased after the first 20 seconds of the cut, suggesting that the process stabilized thermally after the initial transient phase.

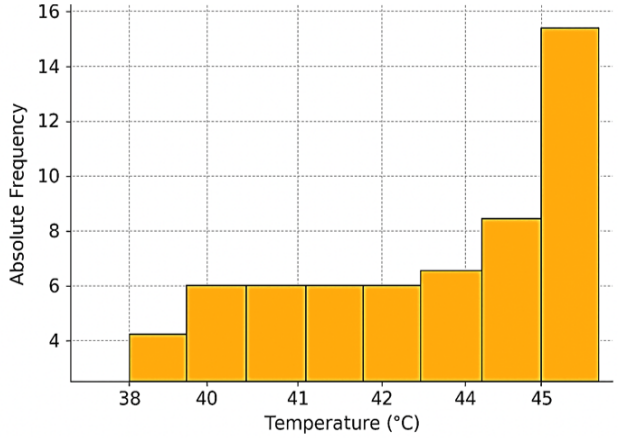

Figure 4: Histogram of cutting temperature values recorded during the necking test.

The cutting speed was modeled as a function of time and diameter. As expected, it decreased continuously during the test due to the reduction in specimen diameter, which contributed to the observed decline in cutting temperature after the peak. 3D plots of Cutting Temperature vs. Diameter and Cutting Speed (Figure 5a) and Cutting Temperature vs. Time and Cutting Speed (Figure 5b) revealed curved surfaces, indicating a peak and subsequent cooling phase illustrated the progressive reduction in temperature and speed as the cut advanced, highlighting the influence of both geometry and velocity on thermal response and corroborating the polynomial temperature behavior over time.

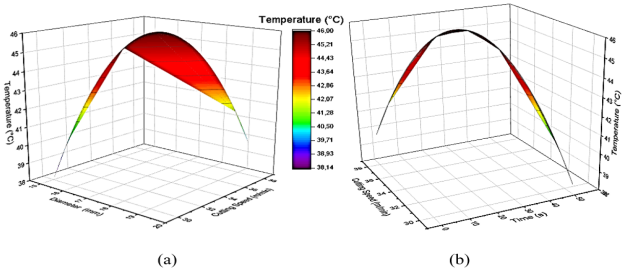

Figure 5: 3D surface plots of cutting temperature: (a) as a function of cutting speed and diameter; (b) as a function of cutting speed and time.

Table 2 shows that cutting temperature values were closely clustered around the mean of 43.55°C, confirmed by the low variance (4.93). The diameter values, also with low variance (1.53), were computed via a linear function, contributing to their consistency. In contrast, cutting speed exhibited a higher variance (1691.00), indicating greater variability during the test. Although derived from diameter, the acceleration of diameter changes over time and affects its variance propagation.

Table 2: Summary Statistics for Measured and Modeled Parameters.

Parameter	Count	Sum	Mean	Variance	Std. Deviation
D (mm)	54	928.81	17.2	1.53	1.24
VC (mm/s)	54	30638.32	567.38	1691	41.12
T (°C)	54	2351.61	43.55	4.93	2.22

Overall, the graphical and statistical results consistently support the interpretation that the thermal regime of the necking test follows a predictable path: rapid rise, stabilization, and controlled decline. The higher variance in cutting speed and its correlation with thermal behavior suggest further exploration with direct speed measurements for more refined modeling.

Conclusion

The results demonstrated a clear non-linear evolution of cutting temperature, characterized by a rapid initial increase, a peak around 46°C, and a subsequent decline as the diameter - and consequently the cutting speed - decreased. Polynomial fitting confirmed the non-linearity of the thermal response, outperforming linear models with coefficients of determination greater than 0.93. These findings highlight the importance of accounting for transient conditions in machinability studies.

Statistical analysis revealed low variance for both temperature and diameter, indicating consistent thermal behavior and geometric modeling. In contrast, the cutting speed presented higher variability, despite being derived from a linear function, suggesting that direct speed measurements could improve the accuracy of future thermal models.

Three-dimensional graphical analysis further clarified the interdependence between temperature, time, diameter, and cutting speed, reinforcing insights from the statistical data. The temperature histogram confirmed the presence of a stable thermal regime, with the highest frequencies concentrated around the peak values.

Acknowledgement

The authors would like to express their gratitude to the Federal University of Pará (UFPA) for providing the infrastructure and institutional support necessary for the development of this research. Special thanks are extended to the Coordination for the Improvement of Higher Education Personnel (CAPES) and the National Council for Scientific and Technological Development (CNPq) for their financial support through research grants and scholarships, which were essential to the execution of this study.

References

1. Geçgel B, Altıntaş Y, Arslan MY, Çelen O, Kocaman E, et al. (2024) Effect of Silicon on Machinability in AlSi6, AlSi12 and AlSi18 Alloys, Silicon 16(4): 1467-1479.
2. Leonidas E, Ayvar SS, Laalej H, Fitzpatrick S, Willmott J (2022) A Comparative Review of Thermocouple and Infrared Radiation Temperature Measurement Methods during the Machining of Metals. Sensors 22(13): 4693.
3. Ueda T, Suzuki K, Shamoto E (2020) Fundamental Study on Cutting Temperature in High Speed Cutting of Difficult-to-Cut Materials. Proceedings of the Machining Innovations Conference (MIC) p. 86-92.
4. Costa T, Dias M, Silva C, Freitas E, Silva A, et al. (2019) Measurement and interrelation of length scale of dendritic microstructures, tensile properties, and machinability of Al-9 wt% Si-(1 wt% Bi) alloys, The International Journal of Advanced Manufacturing Technology 105(1-4): 1391-410.
5. Maciel A, Cosmo N, Souza H, Maués S, Farias A, et al. (2023) Influence of Solidification Parameters and Solute Content on the Machinability of Two Lead-Free Babbit Metals, Current Trends in Engineering Science 3(6): 1-7.
6. Nur Nadirah M, Musfirah A (2024) Optimizing of machining parameters for Hypereutectic Aluminium Silicon Alloys A390 with minimum quantity lubrication in turning using vegetable-based nano fluids. Journal of Physics Conference Series 2907(1).
7. Gabriel P, Gomes L, Spinelli JE (2024) Solidification and Strength Behavior of A356 Al Alloy Wheels, International Journal of Metalcasting 18(4): 3609-3627.
8. Vandersluis E, Emadi P, Andilab B, Ravindran C (2020) The Role of Silicon Morphology in the Electrical Conductivity and Mechanical Properties of As-Cast B319 Aluminum Alloy. Metallurgical and Materials Transactions A 51(4): 1874-1886.
9. Kim T, Lee Z (1997) Time-varying heat transfer coefficients between tube-shaped casting and metal mold. International Journal of Heat and Mass Transfer 40(15): 3513-3525.
10. Chao L, Dianzhong L, Qiang L, Wusheng, Zhenhong W, et al. (2004) Modeling of Solidification of U-2Nb Alloy. Foundry 53(6): 469-471.
11. Silva C, Leal L, Guimarães E, Monteiro JP, Moreira A, et al. (2018) Influence of Thermal Parameters, Microstructure, and Morphology of Si on Machinability of an Al-7.0 wt.% Si Alloy Directionally Solidified. Advances in Materials Science and Engineering.
12. Costa T, Figueiredo G, Silva J, Pinto R, Monteiro JP, et al. (2023) Influence of Lathe Rotation and Secondary Dendritic Arm Spacing on Surface Roughness of an Al-3wt.%Si Alloy Submitted to the Necking Process. Current Trends in Engineering Science 3(2): 1-4.